Sun *et al.* Supplemental Material

1. **Supplemental Table1**
2. **Supplemental Figure Legends**
3. **Supplemental Figures 1-5**

Supplemental Table 1: PCR primers

Gene	Forward primer	Reverse Primer
Bai-1	CGTGTCTGCTCTGGGCCTTTCTTTG	CTCTCCAGCTGGGGTCTCCTTCCAG
Gadd45a	GAGGGAGGGACTCGCACTTGCAATA	GACTCCGAGCCTTGCTGAGCACTTC
p21(Waf-1)	AGACATTCAGAGCCACAGGCACCA	GCATCGCAATCACGGCGCAA
CD133(Prominin-1)	CGAGGACTTTGCACATTCTGGGATAGA	CCAGGGTAGAGGCAAATGTCAGCA
Sox2	ACAACTCCATGACCAGCTCGCAGAC	GCCCTGGAGTGGGAGGAAGAGGTAA
RB	GACAGCGGCCCCGAAGAGCTG	GCCAAGCTCTTTCTCTGACATGATCGGG
SV40-TAg	ACAGTCCCAAGGCTCATTTCAGGCC	GTTTCAGGTTCAGGGGGAGGTGTGG
Cdc6	GCCTCAAACCAGATCCCAGACACAA	TTCTTGCCCAGCTTTGGTGGAGAAC
Bcl2	GGAGAGCGTCAACAGGGAGATGTCA	GTCGCATGCTGGGGCCATATAGTTC
Gapdh	TGGAGTCTACTGGTGTCTTCACCACCAT	GTGGCAGTGATGGCATGGACTGTG

Supplemental Figure Legends

Supplemental Figure 1: Determination of Sex in the TCGA cohort. The "unifiedScaled.txt" file from the analysis by Verhaak *et al.* of The Cancer Genome Atlas (TCGA) data was downloaded. This file includes 202 unique patient specimens in which 22 of 11861 genes are encoded on the Y chromosome (Chr Y). We implemented hierarchical clustering (distance metric=1-Pearson correlation coefficient and average linkage) on the samples based on the 22 Chr Y genes' expression data which were first centered at the median and scaled to have an interquartile range (IQR) of 1. Hierarchical clustering revealed two clusters depicted in the heatmap. The blue to dark purple color spectrum indicates a range of Chr Y gene expression from negative to positive values in the range of -2~2. The left-hand cluster has negative expression for all 22 of the Chr Y genes and represents the FEMALE patients while the right cluster has positive expression and consists of the MALE patients. These clusters are statistically significantly different (p = 2.33e-028) representing 76 female and 126 male patients. The sex assignments were double confirmed using the subset of the samples with RNA-seq data available (data not shown).

Supplemental Figure 2: The PDGF receptor pathway is not potently transforming in male or female *Nf1-/-;DNp53* astrocytes. (**A**) Male and female *Nf1-/-;DNp53* astrocytes were treated with 20 ng/ml PDGF-BB for the times indicated. Cells were harvested and Western blot analysis was performed for PDGF receptor, phosphorylated Akt (pAkt), total Akt, phosphorylated Erk (pErk) and total Erk. Male and female astrocytes express comparable levels of PDGF receptor, and Akt and Erk 1/2 were similarly phosphorylated in both male and female cells in response to PDGF treatment. (**B**) Infrequently, small soft agar colonies were detected in male but not female *Nf1-/-;DNp53* astrocytes treated with PDGF-BB (20ng/ml). Scale bar equals 200 μm. (**C**) Two-by-two contingency table for comparing the rate of PDGF-induced intracranial tumorigenesis with male and female Nf1-/-;DNp53 astrocytes. The trend towards a difference between

tumorigenesis with male and female cells did not reach statistical significance (p=0.2667, Fisher's exact test).

Supplemental Figure 3: The EGFR pathway is equally activated in male and female *Nf1-/-;DNp53* astrocytes. (**A**) Immunohistochemistry (IHC) for EGFR in male and female *Nf1-/-;DNp53* astrocytes. Presence of receptor is indicated by brown stain. There is comparable heterogeneity in levels of EGFR expression regardless of astrocyte sex. No staining was evident in the absence of primary antibody (not shown). (**B**) Phosphorylation of Erk1/2 upon 10 minutes of EGF (50 ng/ml) treatment was detected by IHC and is equally widespread regardless of sex. Scale bar for a and b equals 100 μm. (**C**) Male and female *Nf1-/-;DNp53* astrocytes were treated with 50 ng/ml EGF for the times indicated. Cells were harvested and Western blot analysis was performed for EGFR, actin, phosphorylated Akt (pAkt), total Akt, phosphorylated Erk (pErk) and total Erk. Male and female astrocytes express comparable levels of EGF receptor and exhibit comparable phosphorylation of Akt and Erk 1/2 in response to EGF treatment. (**D**) Quantitation of Western blot data from three independent cultures derived from three independent litters of mice. Male and female EGF responses were not statistically different as determined by two-way ANOVA.

Supplemental Figure 4: Comparisons of male and female intracranial tumors. (**A**) Male and female *Nf1-/-;DNp53* astrocyte derived tumors exhibit similar patterns of intracranial growth. Pictured are representative hematoxylin and eosin stains of male and female tumors as indicated. (**B**) Higher magnification images of male (M) and female (F) tumors demonstrating similar cellular morphologies and densities and secondary structures. Scale bars equal 50 μm. (**C**) No tumor is evident at injection site (asterisk) of an asymptomatic mouse bearing a female implant. (**D**) Representative images of GFP expression at the injection site of an asymptomatic mouse 174 days post-implantation of a female *Nf1-/-;DNp53* astrocytes. Pictured are bright field

(BF) and fluorescence images (GFP) together with the merged image. Arrows indicate the injection site and GFP fluorescence.

Supplemental Figure 5: Map of E2F Reporter Construct. The 3XE2F binding sites were first cloned into pGL4.26 construct, and then the 3XE2F-Luc-SV40-HygR fragment was amplified by PCR. The PCR product was ligated with digested pRRLsinCMV-GFP backbone to replace the CMV-GFP fragment resulting in a lenti-viral E2F-Luc reporter plasmid with a selective marker of hygromycin resistance.

Sun *et al.* Supplemental Figure 1

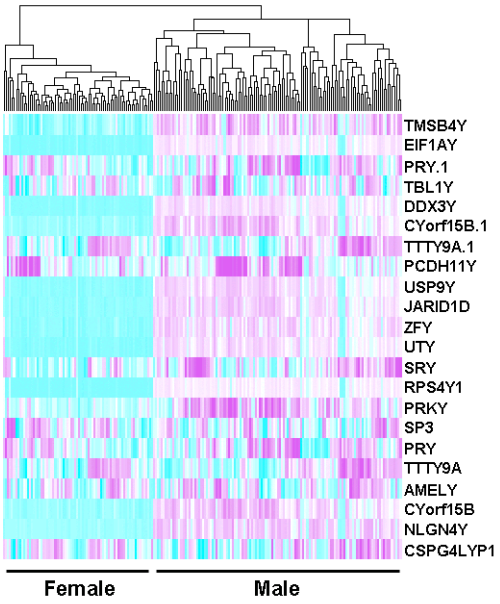

Sun et al. Supplemental Figure 2

A.

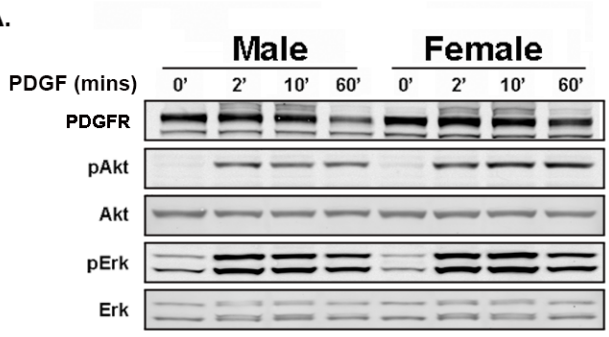

B.

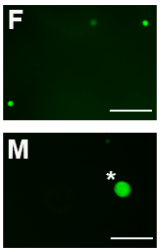

C.

PDGF induced Cortical Tumors

	Tumor	No Tumor
Male	4	3
Female	1	6
Total	5	9

p=0.2667

Sun et al. Supplemental Figure 3

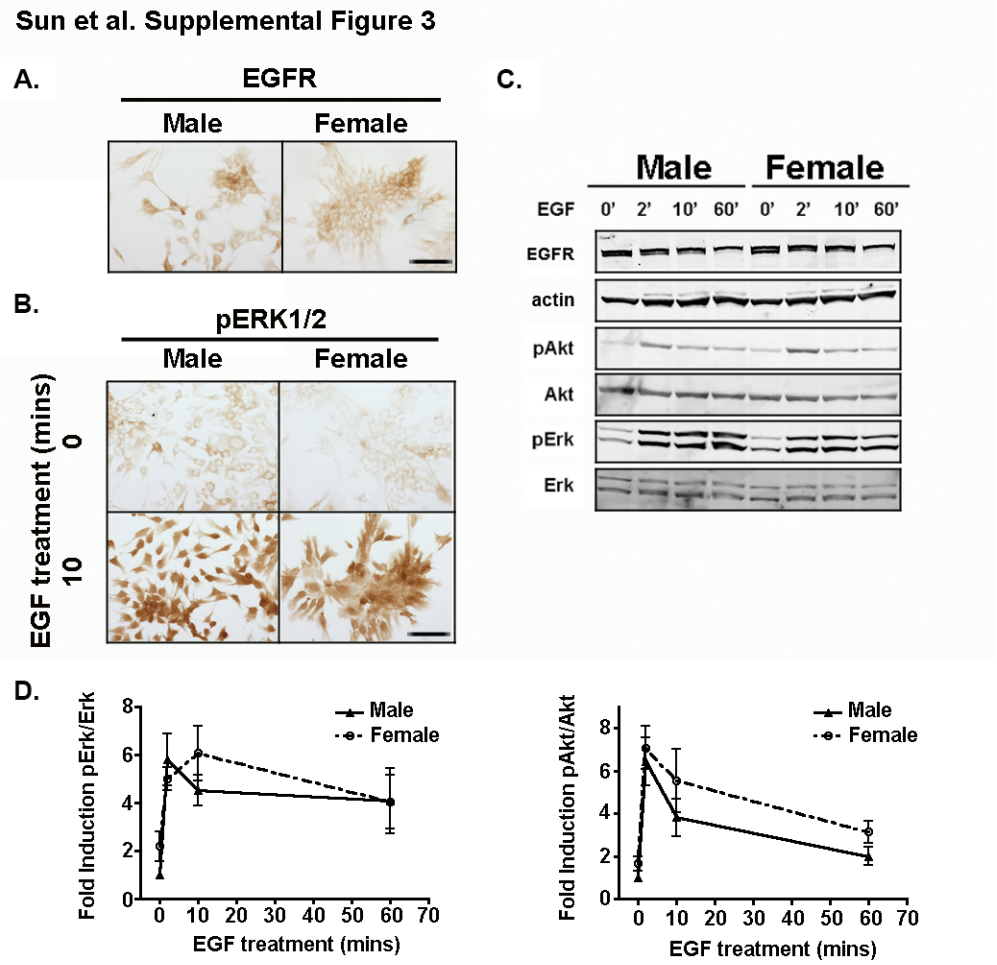

Sun et al. Supplemental Figure 4

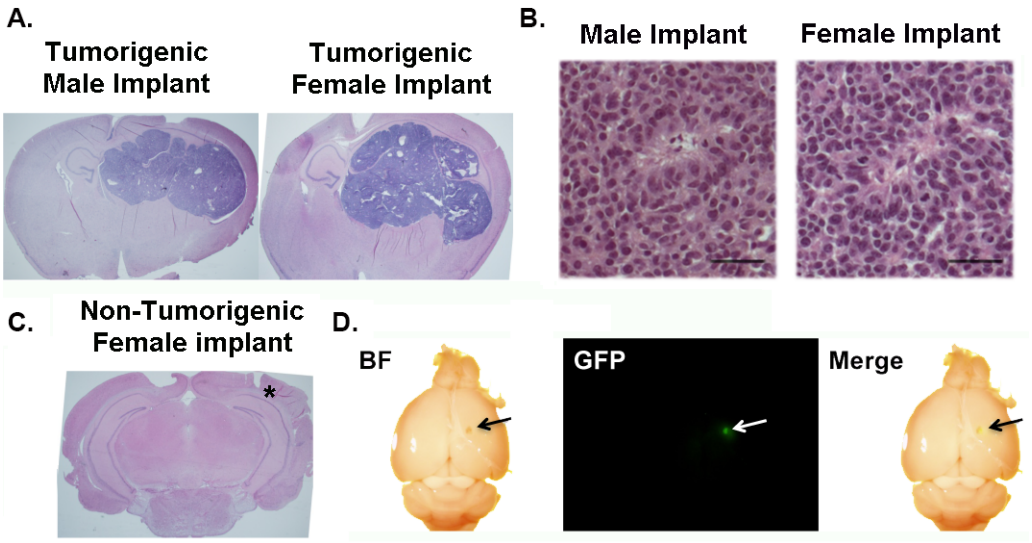

Sun et al. Supplemental Figure 5